Non-Uniform Full-Dimension MIMO: New Topologies and Opportunities

Wendong Liu and Zhaocheng Wang

Abstract

Different from traditional massive MIMO arranging ULA only in the azimuth direction, FD-MIMO offers a practical means of realizing massive MIMO in limited space by equipping URA at the base station, which provides extra spatial degree of freedom in elevation domain and eliminates inter-cell interference considerably. Consequently, FD-MIMO draws much attention from both academia and industry for future 5G wireless communication systems. However, the spectral efficiency of URA is lower than its ULA counterpart when adopting the same number of antenna elements due to low resolution caused by the non-uniform distribution of users in the elevation domain. In this article, the concept of NUFD-MIMO is proposed for the first time, which inherits the advantages and is capable of handling the challenges of traditional FD-MIMO. Structured NURA is designed to enhance the spatial resolution of FD-MIMO in the elevation domain and the corresponding two-dimensional precoding is introduced as well. Moreover, some insights on actual NUFD-MIMO implementations in millimeter-wave systems are provided, including non-uniform multi-beam and two-layer phase shifter feeding network. Finally, future work on the development of NUFD-MIMO is addressed.

Introduction

Massive multiple-input multiple-output (MIMO), equipped with a large-scale antenna array at the base station (BS), is expected to be one of the most promising methodologies to meet the explosively increasing data traffic demands in fifth generation (5G) wireless communications, since it could improve both spectral efficiency and energy efficiency considerably [1]. The low-complexity linear signal processing for massive MIMO systems benefiting from the asymptotic orthogonality when the number of antennas at the BS goes to infinity is also addressed. Nevertheless, it is unrealistic to deploy a huge amount of antenna elements only over the azimuth direction within limited space, which motivates the emergence of full-dimension MIMO (FD-MIMO), also referred to as three-dimension MIMO (3D-MIMO) [2]. Different from traditional massive MIMO arranging uniformly-spaced linear antenna array (ULA) only at the azimuth direction, FD-MIMO employs a large-scale uniformly spaced rectangular antenna array (URA), also known as a uniformly spaced planar antenna array (UPA), which facilitates the installment of a large-scale antenna array within limited space at the BS. Compared to conventional massive MIMO, FD-MIMO offers an extra degree of spatial freedom in the elevation domain and hence is capable of suppressing inter-cell interference. Several advanced 3D processing methodologies, including elevation and azimuth beamforming/precoding, are proposed for FD-MIMO wireless systems [2]. Meanwhile, some key aspects, including 3D channel model, typical application scenarios, antenna configurations and elevation beamforming, have been standardized by the 3rd Generation Partnership Project (3GPP) for LTE/LTE-A [3, 4]. Recently, FD-MIMO has been drawing lots of attention from both academia and industry due to its intrinsic advantages of convenient deployment within a limited space and inter-cell interference elimination.

From the other side, FD-MIMO equipped with URA has lower spectral efficiency than its ULA counterpart with the same number of antenna elements at the BS [2], specifically, low spatial resolution in the elevation domain due to the non-uniform distribution of users is illustrated in [5]. In this article, we propose the concept of non-uniform FD-MIMO (NUFD-MIMO) for the first time, which inherits the advantages of FD-MIMO and is able to handle the inevitable challenges at the same time. Structured non-uniformly spaced rectangular antenna array (NURA) is proposed for FD-MIMO, whereby the antenna elements in the elevation domain are non-uniformly arranged, obeying non-linear functions with adjustable parameters. By selecting proper non-linear functions, the corresponding beamformers/precoders can be designed to improve the spatial resolution in the elevation domain and hence optimize the overall spectral efficiency. After that, several relevant issues are discussed from the perspective of practical implementation of NUFD-MIMO. Specifically, we also introduce two-dimensional precoding and then provide insights on non-uniform multi-beam schemes and two-layer phase shifter feeding networks for NUFD-MIMO in millimeter-wave (mmWave) wireless systems. Finally, conclusions are drawn and the opportunities of adopting NUFD-MIMO in future wireless communications are highlighted.

Overview of FD-MIMO

In this section, we present an overview of FD-MIMO systems. First, URA configuration and 3D beamforming are addressed. Second, the Kro-

Digital Object Identifier:
10.1109/MWC.2019.1800141

Wendong Liu and Zhaocheng Wang (corresponding author) are with Tsinghua University.

1536-1284/19/$25.00 © 2019 IEEE

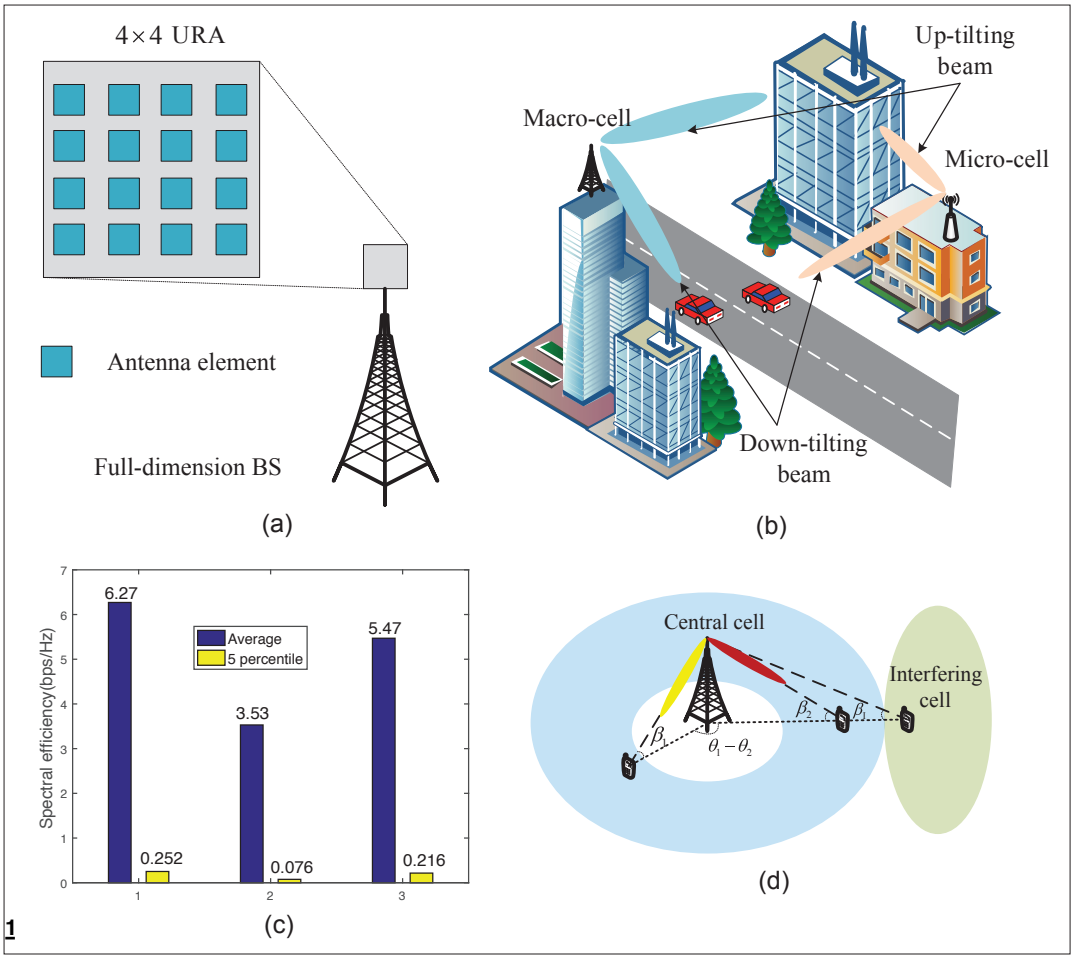

FIGURE 1. a) FD-MIMO with 4 × 4 URA; b) 3D beamforming in macro-cell and micro-cell scenarios; c) performance comparison between 32 × 1 ULA (label 1, $D_A = \lambda/2$) and 8 × 4 URA (label 2, $D_E = D_A = \lambda/2$ and label 3, $D_E = 2\lambda$, $D_A = \lambda/2$).; d) non-uniformity in elevation direction.

necker-product (KP) structure of a three-dimension spatial channel model (3D SCM) is described. After that, KP-based codebook and channel state information (CSI) feedback in FD-MIMO systems are briefed.

URA Configuration and 3D Beamforming

As shown in Fig. 1a, the key feature of conventional FD-MIMO is the adoption of URA at the BS, which overcomes the space limitation in massive MIMO systems when ULA topology is adopted. For example, denoting $M_E = 16$ and $M_A = 16$ as the number of antennas in both the elevation and azimuth domains, the half-wavelength spaced URA occupies about 1.2m × 1.2m area when the carrier frequency is 2GHz. For comparison, almost 19m horizontal distance is required when arranging $M = M_E \times M_A = 256$ antenna elements in ULA from azimuth domain, which is difficult for practical implementation. Moreover, by utilizing a 2D active antenna system (AAS) comprised of gain and phase control components attached to each antenna element, FD-MIMO can produce beams in both the elevation and azimuth domains, referred to as 3D beamforming [6], which provides additional vertical spatial resolution and is capable of distinguishing signals from different angles-of-arrival/departure in the elevation domain (E-AoA/E-AoD) as well as the angles-of-arrival/departure in the azimuth domain (A-AoA/A-AoD). Naturally, FD-MIMO has been regarded as one of the most promising topologies for practical massive MIMO systems, due to its remarkable superiority in arranging a large-scale antenna array at the BS within limited space, supporting high-order multi-user transmissions and reducing inter-cell interference. Consequently, FD-MIMO is capable of improving spectral efficiency considerably and hence draws lots of attention from both academia and industry recently. Figure 1b depicts 3D beamforming application scenarios, such as 3D urban macro cell (3D-UMa) and 3D urban micro cell (3D-UMi) scenarios [3].

Kronecker-Product Structure

Generally, the 3D SCM comprising multi-paths with different E-AoAs/E-AoDs and A-AoAs/A-AoDs is widely utilized [2], which obeys the KP structure. For simplicity, assuming a single antenna is adopted at the user side, we denote $\mathbf{H} \in \mathbb{C}^{M_E \times M_A}$ as the downlink channel matrix between the BS and the user. By performing KP decomposition, $\mathbf{H}$ can be expressed as

$$\mathbf{H} = \sum_{p=1}^{P} \rho_p \mathbf{h}_p^E \otimes \mathbf{h}_p^A, \quad (1)$$

wherein P is the number of multi-paths, ρ_p is the large-scale fading coefficient for the p-th sub-path, $\otimes$ denotes the KP operation, $\mathbf{h}_p^E \in \mathbb{C}^{M_E \times 1}$ and $\mathbf{h}_p^A$

FD-MIMO has been regarded as one of the most promising topologies for practical massive MIMO systems, due to its remarkable superiority in arranging a large-scale antenna array at the BS within limited space, supporting high-order multi-user transmissions and reducing inter-cell interference. Consequently, FD-MIMO is capable of improving spectral efficiency considerably and hence draws lots of attention from both academia and industry.

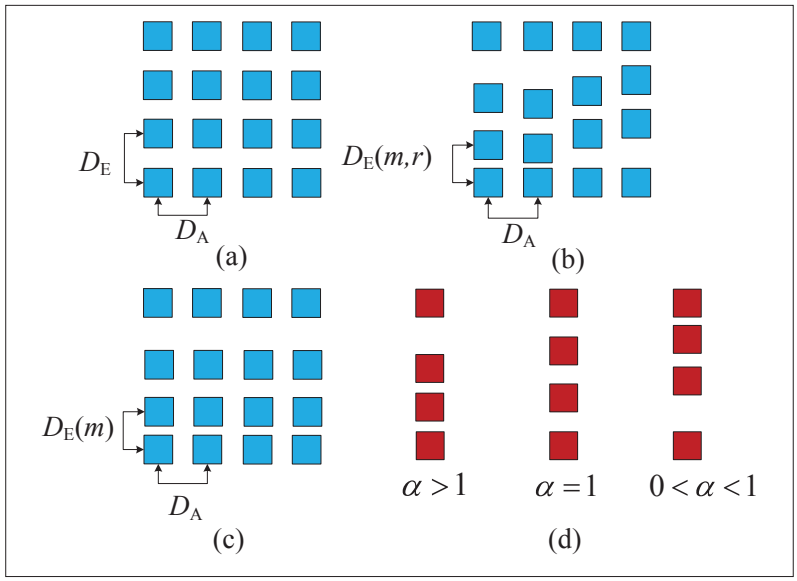

FIGURE 2. Illustration of non-uniformly spaced rectangular array: a) URA; b) unstructured NURA; c) structured NURA; d) distribution of antenna elements in elevation domain with $\alpha < 1$, $\alpha = 1$ and $0 < \alpha < 1$.

$\in \mathbb{C}^{1\times M_A}$ are the channel steering vectors of the p-th sub-path in both the elevation and azimuth domains, which are determined by both E-AoD and A-AoD from the p-th sub-path [2].

Furthermore, considering the modest angular spread of E-AoDs due to few scatters around the highly deployed BS, the multi-path 3D SCM can be approximately simplified to a single-path channel in the elevation domain [7]. Denoting $\mathbf{h}^E \approx \mathbf{h}^E_p$, $p = 1, \cdots, P$ as the approximate single-path steering vector in the elevation domain, the channel matrix can be approximately divided into two parts as $\mathbf{H} \approx \mathbf{h}^E \otimes \Sigma_{p=1}^{P} \rho_p \mathbf{h}^A_p$, which facilitates several low-complexity KP-based signal processing methodologies in FD-MIMO systems [5].

Codebook Design and CSI Feedback

In conventional massive MIMO systems equipped with ULA at the BS, we denote the size of the codebook as L, which represents the number of codewords. In LTE/LTE-A standards, every codeword $\mathbf{w}_l$ is an $M \times 1$ discrete Fourier transformation (DFT) vector. After channel estimation, the user feeds back the index of the best-matched codeword according to the estimated downlink channel state information (CSI), denoted as the precoding matrix indicator (PMI) l, $0 \le l \le L - 1$.

In FD-MIMO systems, the codebook is re-designed based on the KP structure [4]. Specifically, we denote the DFT codeword in the elevation domain as $w_{l_E} \in \mathbb{C}^{M_E\times 1}$, $0 \le l_E \le L_E - 1$ and in the azimuth domain as $\mathbf{w}_{l_A} \in \mathbb{C}^{M_A\times 1}$, $0 \le l_A \le L_A - 1$, wherein L_E and L_A are the number of codewords in both the elevation and azimuth domains, respectively. After that, the final two-dimension DFT (2D-DFT) codeword by the KP operation is calculated as $\mathbf{w}_l = \mathbf{w}_{l_E} \otimes \mathbf{w}^T_{l_A}$. It is apparent that the user selects the best-matched codeword and then feeds back the PMI in both the elevation domain l_E and the azimuth domain l_A, respectively. Therefore, the complexity of channel estimation can be reduced from $\mathbf{O}(L_E \times L_A)$ to $\mathbf{O}(L_E + L_A)$.

Proposed NUFD-MIMO Topology

In conventional FD-MIMO systems, URA and some classic uniform linear signal processing methodologies are utilized. To enhance the performance, NUFD-MIMO is proposed and the cooperative two-dimensional precoding scheme is addressed. In addition, the performance comparison between the proposed NURA with the two-dimensional precoding and its conventional URA counterpart is presented.

FD-MIMO via NURA

This section details the NUFD-MIMO systems equipped with NURA from various perspectives. First, the drawback of FD-MIMO equipped with URA is investigated. Second, the topology of structured NURA and the corresponding modified 3D SCM are illustrated. Next, two different types of structured NURA configurations are demonstrated, including dynamic and static solutions to deploy the NUFD-MIMO systems when a practical implementation is considered. Finally, further discussions on this topic are provided.

Drawback of URA: When the same number of antennas is used at the BS, the spectral efficiency of FD-MIMO equipped with URA is lower than its ULA counterpart. As shown in Fig. 1c, the 32×1 half-wavelength spaced ULA outperforms the 8×4 URA from both downlink average spectral efficiency and 5 percentile spectral efficiency, since low angular resolution in the elevation domain cannot compensate the decrease of resolution from the fewer antenna elements in the azimuth domain [2]. As explained in [5], for downlink transmission, A-AoDs uniformly distribute in $(0, 2\pi)$ due to the uniform locations from mainly outdoor users, which indicates that it is preferred to use ULA and uniform signal processing in the azimuth domain. In contrast, as depicted in Fig. 1d, in typical wireless communication scenarios, the BS is deployed much higher than outdoor users and therefore the E-AoDs distribute non-uniformly in an extremely small angle interval, which can not be distinguished efficiently by URA in the elevation domain. To overcome this issue, non-uniform antenna array topology and non-uniform signal processing are investigated.

Structured NURA: A type of special NURA, called structured NURA, is detailed. Figure 2 illustrates the allocation patterns for 4×4 conventional URA, 4×4 unstructured NURA, and 4×4 structured NURA. For half-wavelength URA depicted in Fig. 2a, the spacings between adjacent antenna elements are constant in both the elevation and azimuth domains, denoted as $D_E = D_A = \lambda/2$. For comparison, two kinds of generic NURA patterns with non-uniformly spaced antenna elements in the elevation domain are depicted in Figs. 2b and 2c, respectively. For unstructured NURA, the antenna spacing in the elevation domain depends on both row index m and column index r. By contrast, the antenna spacing of structured NURA in the elevation domain is only determined by its row index, wherein every elevation sub-array obeys an identical non-uniform distribution. Therefore, the spatial channel model of structured NURA maintains the KP structure, and KP-based 3D beamforming/precoding can be directly extended for NUFD-MIMO systems with structured NURA.

To express the antenna distribution in the elevation domain, a generic non-linear element-positioning function $f(m)$, $0 \le m \le M_E - 1$ is formulated for structured NURA. Under the constraint of occupying the same space in the elevation domain, $f(m)$ is a monotonous increasing function satisfying $0 = f(0) < f(1) < \cdots < f(M_E - 1) = D_E(M_E - 1)$, wherein D_E is the elevation antenna spacing for conventional URA. By selecting various non-linear element-positioning functions, we obtain different structured NURAs. When linear function $f(m) = mD_E$ is preferred, the special case of conventional URA is selected.

Based on the conventional 3D SCM [2], the corresponding channel steering vector $\tilde{\mathbf{h}}_p^E$ should be re-written as follows

$$\tilde{\mathbf{h}}_p^E = \left[1, e^{-j2\pi\frac{f(1)}{\lambda}\sin\beta_p} \cdots e^{-j2\pi\frac{f(m)}{\lambda}\sin\beta_p} \cdots e^{-j2\pi\frac{f(M_E-1)}{\lambda}\sin\beta_p}\right]^T \quad (2)$$

wherein λ is the wavelength, and β_p is the E-AoD of the p-th sub-path. Combined with the azimuth channel steering vector $\mathbf{h}_p^A$, the modified 3D channel matrix $\tilde{\mathbf{H}}$ can be obtained by replacing $\mathbf{h}_p^E$ in Eq. 1 as $\tilde{\mathbf{h}}_p^E$. Consequently, the 3D beamforming/precoding vectors and the signal-to-interference plus noise ratio (SINR) related to the channel models are modified as well. By properly exploring the non-linear element-positioning function $f(m)$ and designing the structured NURA pattern, the spatial resolution in the elevation domain could be improved and hence the system's spectral efficiency could be enhanced considerably.

To provide an intuitive description of structured NURA, three kinds of non-linear element-positioning functions, power-exponent, exponential, and tangent functions, are introduced in [5], wherein every non-linear function contains an adjustable non-linear scaling factor (e.g., α) to control its exact function form. Choosing the power-exponent element-positioning function as an example, we have

$$f_\alpha(m) = \frac{D_E m^\alpha}{(M_E - 1)^{\alpha-1}} \quad (3)$$

wherein $0 \le m \le M_E - 1$, which is specified by the adjustable exponent parameter $\alpha > 0$. Figure 2d illustrates the distribution patterns of antenna elements in the elevation domain with $0 < \alpha < 1$, $\alpha = 1$ and $\alpha > 1$. Specifically, structured NURA becomes conventional URA with the exponent $\alpha = 1$.

Dynamic or Static Configurations: Generally, the non-linear scaling factor is mainly affected by the distribution of users as well as the relative height between users and the BS. To optimize the performance of NUFD-MIMO systems with structured NURA, dynamic and static configurations are illustrated. Without the loss of generality, the power-exponent element positioning function $f_\alpha(m)$ is utilized at the BS.

For the dynamic configured NURA (DC-NURA), the parameter α varies periodically with the channel state to maximize the instantaneous spectral efficiency. Consequently, the optimal $f_\alpha(m)$ and the structured NURA configuration have to be adjusted continuously, which requires innovative manufacturing technologies. Although this kind of reconfigurable antenna array has not yet been adopted in current wireless communication standards, DC-NURA provides the upper-bound of achievable spectral efficiency for NUFD-MIMO equipped with structured NURA. Recently, several potential research works have produced various new-type antennas, such as a liquid metal antenna [8], which is capable of reconfiguring the antenna structure during the operational stage and hence offers a promising solution for implementing our proposed DC-NURA. Moreover, when channel coherence time becomes sufficiently long, the implementation of DC-NURA might be feasible in practical NUFD-MIMO systems.

In contrast, for the static configured NURA (SC-NURA), the antenna elements are pre-fixed to optimize the long-term expectation of average spectral efficiency including numerous various channel state realizations, which depends on the underlying channel model distribution. Since the antenna elements for SC-NURA are kept unchanged during operation stage, it is entirely practical in current NUFD-MIMO systems with the increased spectral efficiency.

Further Discussions: Hereby we provide further discussions in order to highlight the interesting opportunities offered by NURA architecture. First, the mutual coupling between adjacent antenna elements, which might dramatically affect system performance, is ignored, especially with smaller antenna spacing between adjacent antenna elements in NURA configurations. Therefore, more elaborate research on NURA in consideration of mutual coupling should be further investigated.

Second, the non-uniform multi-panel structure is acknowledged in the 3GPP standard [9], which can be regarded as a special case of structured NURA. Different from the uniform multi-panel depicted in Fig. 3a, the spacing between adjacent panels $D_{edge,E}$ and $D_{edge,A}$ are larger than the spacing between adjacent antenna elements D_E and D_A in the same panel, as shown in Fig. 3b, which could provide further design freedom in multi-panel wireless systems.

Besides the proposed structured NURA, many variations of non-uniform antenna arrays for different application scenarios need to be considered [10]. For example, as shown in the left of Fig. 3c, a cylinder array could provide better coverage with the sacrifice of beamforming gain and beam width. Instead of cylinder or rectangular configurations, a segmented array, as depicted in the right of Fig. 3c, could also achieve good trade-off between required coverage and beamforming gain. Together with carefully designed new-type non-uniform antenna array structures, NUFD-MIMO could acquire its intrinsic all-around benefits compared with its conventional FD-MIMO counterpart.

Two-Dimensional Precoding

Conventional precoding methods, such as zero-forcing (ZF) precoding and matched-filter (MF) precoding, are performed on the 3D channel matrix $\mathbf{h}_{vec} = \text{cvec}(\mathbf{H}) \in \mathbb{C}^{M_E M_A \times 1}$, which suffers from inter-cell interference in multi-cell scenarios due to pilot contamination, wherein the KP structure of 3D SCM is not fully exploited. To cope with inter-cell interference, the authors in [11] propose low-complexity two-dimensional precoding based

To enhance the performance, NUFD-MIMO is proposed and the cooperative two-dimensional precoding scheme is addressed. In addition, the performance comparison between the proposed NURA with the two-dimensional precoding and its conventional URA counterpart is presented.

mmWave has been deemed as an attractive candidate methodology for 5G wireless communications because of its abundant bandwidth. Due to its shorter wavelength, more antenna elements can be packed into limited space. Moreover, the severe path-loss of mmWave signals can be compensated by the beamforming gain along with the massive MIMO technique.

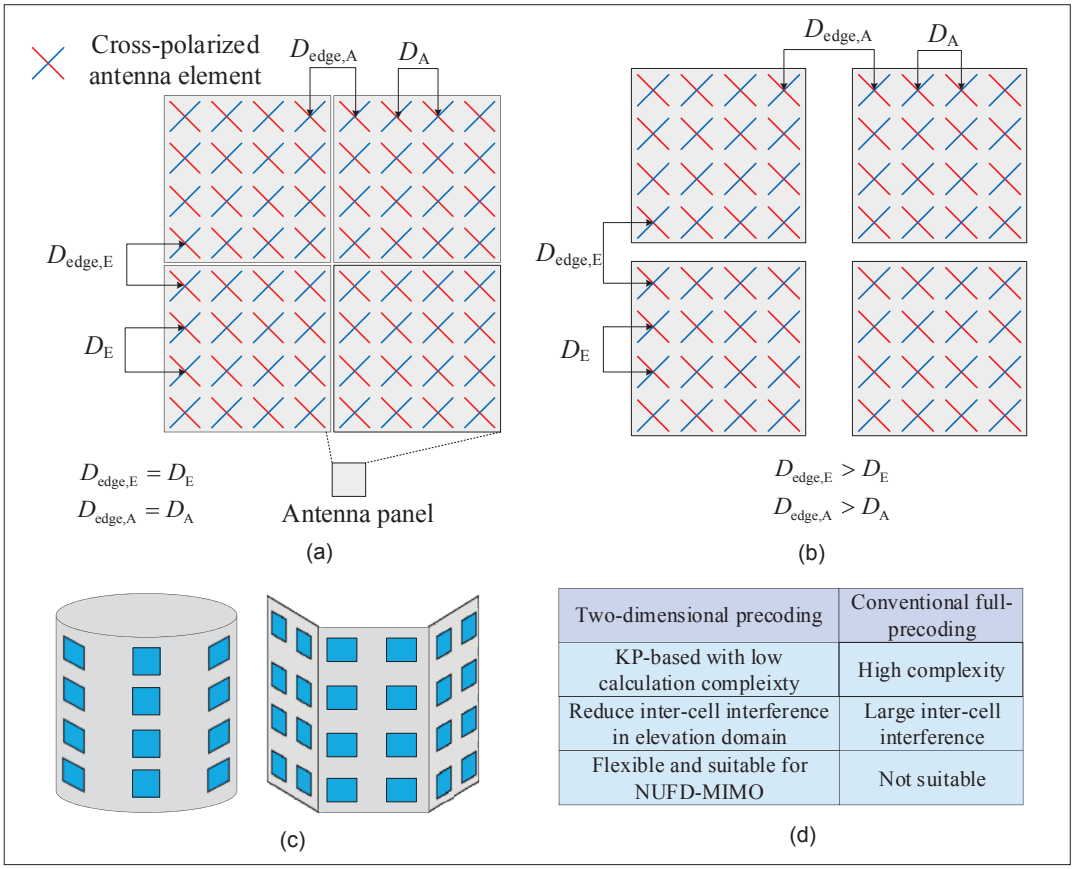

Two-dimensional precoding	Conventional full-precoding
KP-based with low calculation compleixty	High complexity
Reduce inter-cell interference in elevation domain	Large inter-cell interference
Flexible and suitable for NUFD-MIMO	Not suitable

FIGURE 3. Different antenna array structures: a) uniform multi-panel structure; b) non-uniform multi-panel structure; c) cylinder and segmented array; d) advantages of two-dimensional precoding over conventional full-precoding.

on the KP structure of 3D SCM to further enhance the performance of NUFD-MIMO systems. Next, we will detail the procedure of two-dimensional precoding, which can be divided into four steps.

Step 1: Utilizing the approximately KP-decomposed channel model mentioned previously, we construct the elevation channel matrix $\mathbf{H}_E \in \mathbb{C}^{K\times M_E}$, whereby its k-th column $\mathbf{h}_k^E$ indicates the elevation channel steering vector for the k-th user. Using ZF precoding as an example, we perform the elevation ZF precoding as $\mathbf{P}_E = \mathbf{H}_E^H(\mathbf{H}_E\mathbf{H}_E^H)^{-1}\Gamma_E$, wherein Γ_E is a diagonal power normalization matrix. Meanwhile, the k-th column of $\mathbf{P}_E$, denoted as $\mathbf{p}_k^E$, represents the elevation precoder for the k-th user.

Step 2: Calculate the equivalent azimuth channel steering vector for the k-th user as $\mathbf{h}_k^A = \mathbf{H}_k^T\mathbf{p}_k^E$, wherein $\mathbf{H}_k$ is the 3D channel matrix between the BS and the k-th user.

Step 3: Similarly, the equivalent azimuth channel matrix $\mathbf{H}_A \in \mathbb{C}^{K\times M_A}$ is constructed and its k-th column is given by $\mathbf{h}_k^A$. Then we perform ZF precoding on the equivalent azimuth domain as $\mathbf{P}_A = \mathbf{H}_A^H(\mathbf{H}_A\mathbf{H}_A^H)^{-1}\Gamma_A$, wherein Γ_A is the diagonal power normalization matrix and $\mathbf{p}_k^A$, referred to the k-th column of $\mathbf{P}_A$, is the azimuth precoder for the k-th user.

Step 4: Finally, the overall precoder matrix for the k-th user is constructed as $\mathbf{P}_k = \mathbf{p}_k^E \otimes (\mathbf{p}_k^A)^T$.

As listed in Fig. 3d, two-dimensional precoding is extremely appropriate for NUFD-MIMO systems with structured NURA, since the elevation precoding is independently pre-performed at Step 1, which effectively takes advantage of the non-uniform elevation characteristic, and hence reduces the intra-cell interference as well as the inter-cell interference in the elevation domain. When utilizing structured NURA at the BS, we only need to substitute $\tilde{\mathbf{h}}_k^E$ formulated in Eq. 1 (leaving out the subscript p in the approximately KP-decomposed channel model) for $\mathbf{h}_k^E$ in Step 1, and non-uniform precoding can be conducted smoothly in the elevation domain.

Simulation Results

When two-dimensional precoding in NUFD-MIMO systems with structured NURA is adopted, simulation results are presented to verify the superiority of two-dimensional precoding and our novel structured NURA. Some basic simulation parameters are shown in Fig. 4d, wherein the outdoor user scenarios are mainly considered. Hereby we use the power-exponent element-positioning function $f\alpha(m)$ as an example.

First, we concentrate on the performance of two-dimensional precoding in FD-MIMO systems with conventional URA. As shown in Fig. 1d, benefited from the 3D channel characteristics that the E-AoDs of the signals from interfering cells are much smaller than those of the center cell ($\beta_1 < \beta_2$), inter-cell interference can be pre-reduced in the elevation domain at Step 1. Simulation results in Fig. 4a show that two-dimensional precoding outperforms the traditional 3D beamforming and the conventional full-precoding method ignoring KP structure on downlink spectral efficiency in multi-cell scenarios. Moreover, with smaller angular

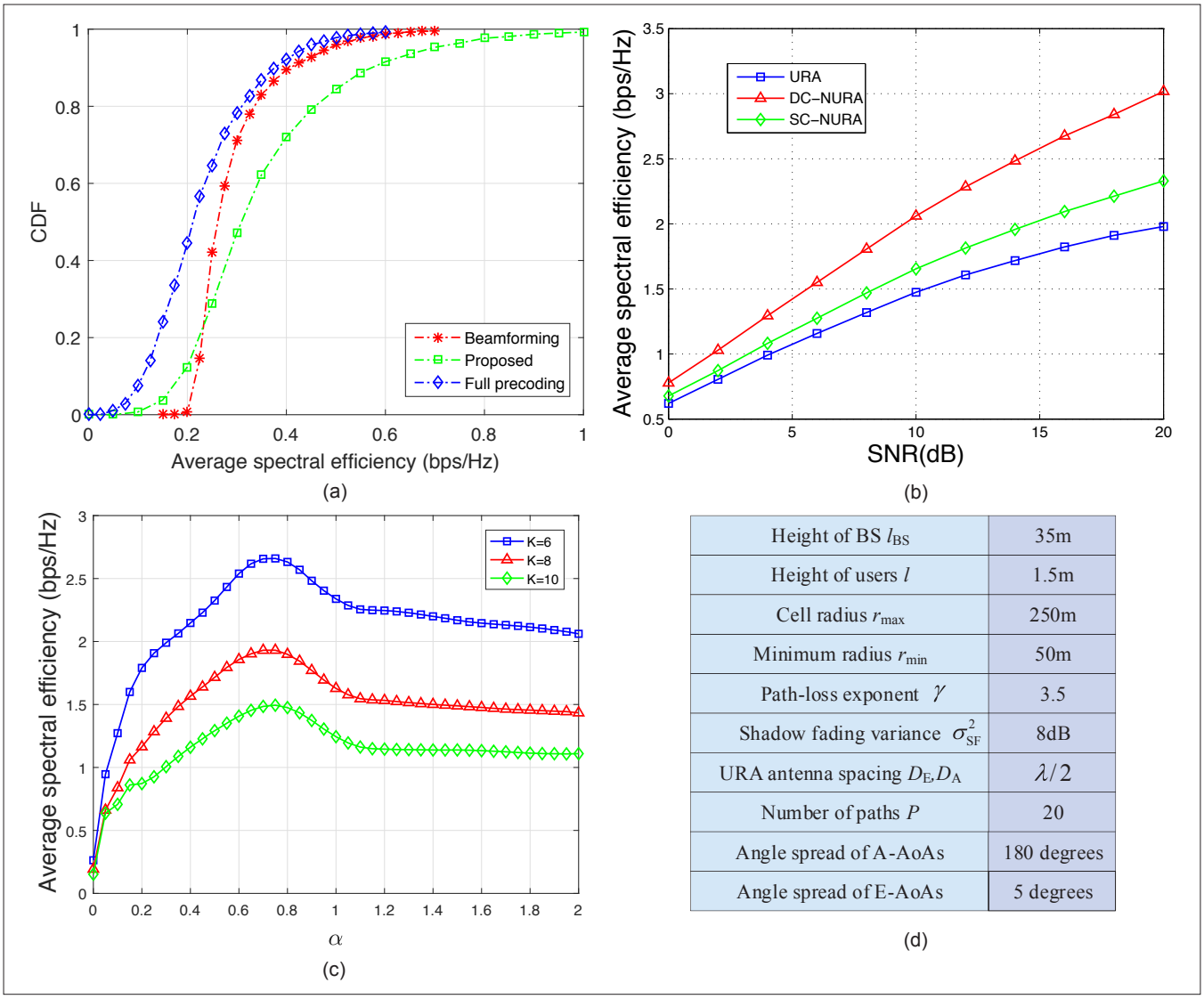

Height of BS l_{BS}	35m
Height of users l	1.5m
Cell radius r_{max}	250m
Minimum radius r_{min}	50m
Path-loss exponent γ	3.5
Shadow fading variance σ_{SF}^2	8dB
URA antenna spacing D_E, D_A	$\lambda/2$
Number of paths P	20
Angle spread of A-AoAs	180 degrees
Angle spread of E-AoAs	5 degrees

FIGURE 4. Performance evaluations: a) CDF comparison of average spectral efficiency with different precoding schemes in multi-cell scenario; b) average spectral efficiency comparison among SC-NURA, DC-NURA and URA in different SNRs; c) performance of SC-NURA with $0 < \alpha < 2$ and $K = 6, 8, 10$; d) basic simulation parameters.

spread of E-AoD, the approximate KP-decomposed channel model from before would be more accurate and hence the performance of two-dimensional precoding will be further increased. Next, when utilizing structured NURA, the average spectral efficiency comparison among URA, SC-NURA and DC-NURA with different SNRs is depicted in Fig. 4b. Obviously, both NURA designs outperform the conventional URA considerably.

Figure 4c depicts the average spectral efficiency as the function of α with the number of users $K = 6, 8, 10$ and the array size of $M_E \times M_A = 64 \times 64$. Obviously, the spectral efficiency has a single peak around $\alpha = 0.7$, which demonstrates that the optimal design of SC-NURA with the power-exponent element-positioning function $f_{\alpha=0.7}(m)$ significantly outperforms the URA design with $\alpha = 1$. Moreover, observed from Fig. 4c, the optimal α only changes slightly with a different numbers of users. It is indicated that we do not have to re-adjust the structure of SC-NURA to support various numbers of users per resource block during the network operational stage. Further comprehensive simulation results have been given in [5], which reveals the superiority of NUFD-MIMO systems with structured NURA explicitly.

NUFD-MIMO in MmWave Communications

As we know, mmWave has been deemed as an attractive candidate methodology for 5G wireless communications because of its abundant bandwidth. Due to its shorter wavelength, more antenna elements can be packed into limited space. Moreover, the severe path-loss of mmWave signals can be compensated by the beamforming gain along with the massive MIMO technique. Therefore, the combination of mmWave and massive MIMO, especially FD-MIMO, should be extensively explored. As discussed above, the proposed structured NURA and two-dimensional precoding can greatly enhance the performance of current FD-MIMO systems. In this section, several relevant issues, including non-uniform multi-beam schemes and two-layer phase shifter feeding networks are discussed to facilitate the usage of NUFD-MIMO in mmWave wireless communication systems.

As part of our future work, possible precoding methodologies would be investigated for different non-uniform antenna array topologies. Moreover, for NUFD-MIMO in mmWave communications, proper non-uniform multi-beam pattern and training schemes would be further explored and evaluated for various application scenarios.

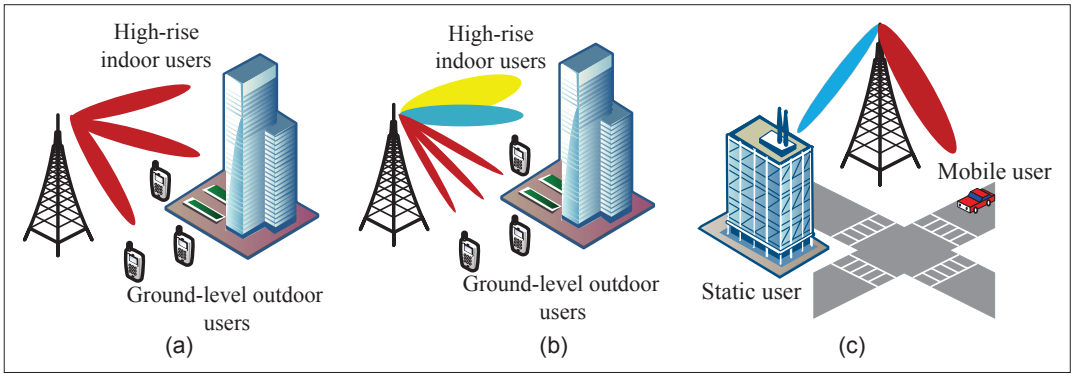

FIGURE 5. Multi-beam pattern comparison: a) conventional uniform multi-beam pattern; b) non-uniform multi-beam pattern for ground-level outdoor users and high-rise indoor users; c) non-uniform pattern for static and mobile users.

Non-Uniform Multi-Beam Methodology

In mmWave communications, BS provides multiple sharp beams via the massive MIMO technique to achieve sufficient beamforming gain and compensate the prominent propagation pathloss. In order to establish the beam pair link, the beam training procedure is required, wherein the user feeds back the beam index to the BS having the best reception quality among all candidate beams. After that, the BS selects the corresponding beam for data transmission. Generally, sharp beams at the BS guarantee the beam coverage and the reception quality of the wireless signals, but lead to severe beam training overhead and hence the loss of spectral efficiency. In contrast, beam training overhead can be reduced significantly by adopting fewer wide beams at the BS, which sacrifices the beam coverage and reception quality. Therefore, a good trade-off between the beam coverage and beam training overhead is an important issue, which requires a carefully designed multi-beam pattern and beam training methodology.

Non-Uniform Beam Pattern: As shown in Fig. 5a, conventional multi-beam schemes provide a uniform beam pattern, wherein all beams use uniformly-quantized beam vectors and have the same beamwidth. However, users stay practically in non-uniform distribution around the BS. Specifically, users are mostly located at ground-level instead of in high-rise buildings, which indicates that in typical FD-MIMO cellular systems, the beams oriented to the ground are most frequently selected. In contrast, the beams pointed to the high-rise indoor users are utilized less frequently. Such non-uniformity causes a waste of spatial resources, which motivates us to investigate the non-uniform beam pattern.

A simple non-uniform beam pattern is depicted in Fig. 5b, wherein the beam directions are non-uniformly quantized. More and sharper beams are directed to the ground, but fewer and wider beams are directed toward the high-altitude. By way of proper beam and user scheduling, a non-uniform beam pattern could improve the service quality for ground-level users and hence the spatial resources could be more efficiently explored.

Moreover, non-uniform beams can support various services. For example, as shown in Fig. 5c, sharp beams are utilized to provide high data rate for static users without frequent beam switching, but wide beams are preferred in mobile vehicle communications to reduce the frequency of beam switching and ensure the robustness of data transmission.

Non-Uniform Smart Beam Training: In addition to a non-uniform beam pattern, non-uniform beam training methods should be investigated as well. Generally, uniform beam sweeping is adopted, wherein the candidate beams are sequentially utilized for the transmission of reference signals [12]. Generally, assuming N beams at the BS and omni-directional reception at users, we have to spend N time slots for beam sweeping, which leads to high beam training overhead when N becomes large in mmWave massive MIMO systems.

In order to reduce the large beam training overhead, a non-uniform beam training strategy is proposed, wherein the priori information of utilization frequency for candidate beams and out-of-band location information, such as GPS positioning, are considered. Specifically, several out-of-range beams can be pre-eliminated based on the location information and remaining candidate beams should be swept according to the descending order of recorded utilization frequency at the BS. In addition, the beam training procedure stops when users find the beam that provides sufficient link quality. Consequently, the average beam training overhead would be greatly reduced. For example, in practical NUFD-MIMO systems, beams oriented to the ground may be used frequently, which should be first tested to ensure that most users can be served with lower access latency.

In summary, a non-uniform beam pattern and smart beam training schemes are the promising aspects to further explore the potential of NUFD-MIMO topology in mmWave communications, which attracts much attention from both academia and industry.

Two-Layer Phase Shifter Feeding Network

In order to reduce the hardware complexity and power consumption, a hybrid architecture comprising digital and analog parts is considered as the primary topology to replace the full-digital transmitter in mmWave systems [13], wherein the full-connection and sub-connection structures are mainly studied. Combined with FD-MIMO, a two-layer phase shifter feeding network is introduced [14]. As illustrated in Fig. 6a, the novel architecture consists of a hor-

izontal phase shifter layer and a vertical phase shifter layer, wherein every antenna element is connected with a vertical phase shifter and every column of vertical phase shifters are fully connected to an individual radio frequency (RF) chain through a horizontal phase shifter. By developing the corresponding iterative hybrid precoding algorithm, the proposed two-layer architecture can approach the full-connection one on spectral efficiency with small vertical angle-spread and possess much reduced hardware complexity.

In conclusion, this two-layer architecture achieves the trade-off between spectral efficiency and hardware complexity compared with conventional full-connection and sub-connection architectures. Specifically, the phase shifter resource comparison is listed in Fig. 6b, wherein K is the number of RF chains and $KM_E + M_EM_A$ phase shifters are adopted in the proposed architecture. Moreover, the two-layer phase shifter feeding network decouples the vertical and horizontal connections, which facilitates the design of non-uniform antenna arrays as well as non-uniform beam patterns in elevation direction and provides some insights on the actual design of a transmitter architecture in NUFD-MIMO systems. Since [14] only investigates the two-layer architecture with ideal continuous phase shifters, b-bit (e.g., b = 1, 2 and 3) quantized phase shifters are widely used in practical implementations to reduce the hardware complexity. The quantization error results in the decrease of phase control accuracy with sidelobes, and hence the precoding/beamforming performance. Further quantization effects can be detailed in [15].

Conclusions and Future Work

In this article, various aspects of NUFD-MIMO are illustrated, including non-uniform antenna array design, two-dimension precoding, non-uniform multi-beam and two-layer phase shifter feeding networks in mmWave communication systems. First, we proposed the topology of structured NURA, and demonstrated its superior performance with the corresponding two-dimensional precoding on the spectral efficiency compared to the conventional URA. Second, we highlighted insights on actual NUFD-MIMO implementation in mmWave wireless communications. Specifically, a non-uniform beam pattern and the relevant beam training are provided in order to acquire the trade-off between beam coverage and training overhead. Moreover, a two-layer phase shifter feeding network is introduced. It is expected that NUFD-MIMO will play an important role and attract much attention in future 5G wireless communications.

As part of our future work, possible precoding methodologies would be investigated for different non-uniform antenna array topologies. Moreover, for NUFD-MIMO in mmWave communications, proper non-uniform multi-beam pattern and training schemes would be further explored and evaluated for various application scenarios, such as secure communication, unmanned aerial vehicular (UAV)-based communication and low-latency communication, wherein more comprehensive analytical and numerical results would be presented.

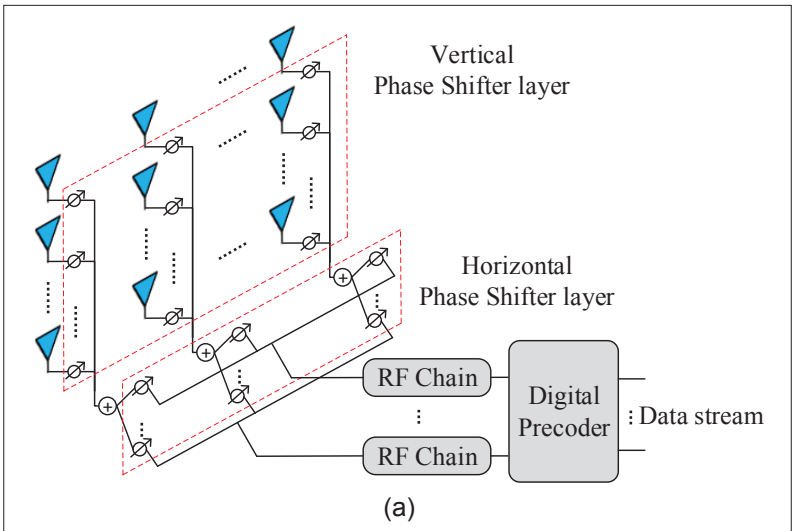

(a)

Number of required phase shifters	8×8 URA		16×16 URA	
	K=2	K=4	K=4	K=8
Two-layer phase shifter feeding network	80	96	320	384
Sub-connection	64	64	256	256
Full-connection	128	256	1024	2048

(b)

FIGURE 6. a) Two-layer phase shifter feeding network; b) phase shifter resource comparison.

Acknowledgment

This work was supported in part by the National Natural Science Foundation of China (Grant No. 61571267 and 61711530244); in part by the Shenzhen Fundamental Research Project (JCYJ20170817160741066); in part by the Guangdong Optical Wireless Communication Engineering and Technology Center; and in part by the Shenzhen Wireless over VLC Technology Engineering Lab Promotion.

References

[1] F. Rusek *et al.*, "Scaling Up MIMO: Opportunities and Challenges with Very Large Arrays," *IEEE Signal Process. Mag.*, vol. 30, no. 1, Jan. 2013, pp. 40–60.
[2] Y.-H. Nam *et al.*, "Full-Dimension MIMO (FD-MIMO) for Next Generation Celluar Technology," *IEEE Commun. Mag.*, vol. 51, no. 6, June 2013, pp. 172–79.
[3] 3GPP TR 36.873, "Study on 3D Channel Model for LTE."
[4] 3GPP TR 36.897, "Study on Elevation Beamforming/Full-Dimension (FD) MIMO for LTE."
[5] W. Liu *et al.*, "Structured Non-Uniformly Spaced Rectangular Array Design for FD-MIMO Systems," *IEEE Trans. Wirel. Commun.*, vol. 16, no. 5, Mar. 2017, pp. 3252–66.
[6] 3GPP TR 37.840, "Study of Radio Frequency (RF) and Electromagnetic Compatibility (EMC) Requirements for Active Antenna Array System (AAS) Base Station."
[7] A. Kammoun *et al.*, "Preliminary Results on 3D Channel Modeling: From Theory to Standardization," *IEEE JSAC*, vol. 32, no. 6, June 2014, pp. 1219–29.
[8] M. Wang *et al.*, "A Reconfigurable Liquid Metal Antenna Driven by Electrochemically Controlled Capillarity," *J. Appl. Phys.*, vol. 117, no. 19, 2015, pp. 194901-1–194901-5.
[9] 3GPP TSG RAN WG1 Meeting #88 R1-1702196 "On Multi-TRP and Multi-Panel Transmission."
[10] M. Agiwal, A. Roy, and N. Saxena, "Next Generation 5G Wireless Networks: A Comprehensive Survey, " *IEEE Commun. Surveys & Tut.*, vol. 18, no. 3, 3rd Quart. 2016, pp. 1617–55.

[11] Z. Wang *et al.*, "Two-Dimensional Precoding for 3-D Massive MIMO," *IEEE Trans. Vehi. Technol.*, vol. 66, no. 6, pp. 5488–5493, June 2017.
[12] V. Raghaven *et al.*, "Beamforming Tradeoffs for Initial UE Discovery in Millimeter-Wave MIMO Systems," *IEEE JSAC*, vol. 10, no. 3, Apr. 2016, pp. 543–59.
[13] O. El Ayach *et al.*, "Spatially Sparse Precoding in Millimeter Wave MIMO Systems," *IEEE Trans. Wirel. Commun.*, vol. 13, no. 3, Mar. 2014, pp. 1499–1513.
[14] P. Zhao *et al.*, "Hybrid Precoding with Two-Layer Phase Shifter Feeding Network for Mmwave FD-MIMO Systems," *IEEE Globecom 2017*, Singapore, Dec. 2017.
[15] Y.-P. Lin, "On the Quantization of Phase Shifters for Hybrid Precoding Systems," *IEEE Trans. Signal Process.*, vol. 65, no. 9, May 2017, pp. 2237–46.

Biographies

WENDONG LIU (lwd15@mails.tsinghua.edu.cn) received the B.S. degree (Hons.) from Tsinghua University, Beijing, China, in 2015. He is currently pursuing the Ph.D. degree with the Department of Electronic Engineering, Tsinghua University. His research interests include massive MIMO, full-dimension MIMO and millimeter-wave communications.

ZHAOCHENG WANG [M'09, SM'11] (zcwang@tsinghua.edu.cn) received the B.S., M.S., and Ph.D. degrees from Tsinghua University, Beijing, China, in 1991, 1993, and 1996, respectively. From 1996 to 1997, he was a postdoctoral fellow with Nanyang Technological University, Singapore. From 1997 to 1999, he was with OKI Techno Centre (Singapore) Pte. Ltd., Singapore, where he was first a research engineer and later became a senior engineer. From 1999 to 2009, he was with Sony Deutschland GmbH, where he was first a senior engineer and later became a principal engineer. He is currently a professor of electronic engineering with Tsinghua University and serves as the Director of the Broadband Communication Key Laboratory, Tsinghua National Laboratory for Information Science and Technology (TNlist). He has authored or coauthored over 120 journal papers. He is the holder of 34 granted U.S./EU patents. He coauthored two books, one of which, *Millimeter Wave Communication Systems*, was selected by the IEEE Series on Digital and Mobile Communication (Wiley-IEEE Press). His research interests include wireless communications, visible light communications, millimeterwave communications, and digital broadcasting. He is a Fellow of the Institution of Engineering and Technology. He served as an associate editor of *IEEE Transactions on Wireless Communications* (2011–2015) and an associate editor of *IEEE Communications Letters* (2013–2016), and has also served as Technical Program Committee Co-Chair of various international conferences.